Journal of Aircraft

VOLUME 8 OCTOBER 1971 NUMBER 10

Some Considerations Relative to the Prediction of Unsteady Air Loads on Lifting Configurations

HOLT ASHLEY*
Stanford University, Stanford, Calif.

A personal viewpoint is offered on several fundamental issues whose understanding is expected to contribute to improved unsteady lifting surface and interference theory. The position is adopted that the subject under discussion should properly include control surfaces and similar devices which create slope discontinuities or gaps in the geometry of otherwise nearly-planar lifting systems. The first question addressed is that of loading singularities inherent in linearized potential theory. They are classified as 1) local, in the sense that both the nature and magnitude of the singularity are determined by boundary conditions in the "inner field"; or 2) global, in the sense that the entire boundary value problem must be solved to determine their details. Available results are reviewed relative to discontinuities in surface slope, planform shape, dihedral angle, etc., and suggestions are offered for combining them into numerical solution schemes. With respect to the analysis of interfering lifting surfaces, selected recent activity on continuous solution of various subsonic and supersonic cases is described.† Regarding the area-element or "box" approach to the latter, it is recommended that an element in the form of a trapezium, similar to that employed by Woodward for steady flow, will also improve the behavior of predicted loads for oscillatory motion of interacting surfaces. Formulas for certain of the required influence coefficients are developed. Finally some nonlinear effects are examined which are felt to have greater significance for interference problems than for isolated lifting wings. These phenomena include the normal displacement and self-deformation of wakes which induce loads on aft surfaces, the local influences of profile thickness and displacement due to boundary layer growth.

I. Introduction

SUBSTANTIAL effort has been devoted during the past two or three years toward the practical application of linearized unsteady aerodynamic theory for interfering lifting surfaces at both subsonic and supersonic flight speeds. Much of this effort has been successful, in the sense that generalized forces can, in many cases, be calculated with sufficient accuracy for routine aeroelastic analyses. Yet it would be well to recall the long history of development of unsteady aerodynamics for simple planar lifting surfaces and to appreciate the many refinements which gradually led to increased efficiency and accuracy in detail over the first generation of "exact numerical solutions." With a second generation of interference theories now on the horizon, the author hopes to offer a personal viewpoint on several issues whose understanding is expected to contribute such improvements.

Received February 5, 1971; revision received July 1, 1971. Research supported by USAF Office of Scientific Research under Contract F44620-68-C-0036. This paper is adapted from a talk delivered to the AGARD Symposium on Unsteady Aerodynamics for Aeroelastic Analysis of Interfering Surfaces, Tønsberg, Norway, November 1970.

Index categories: Airplane and Component Aerodynamics; Nonsteady Aerodynamics.

* Professor, Aeronautics and Astronautics, Stanford University, Stanford, Calif. Fellow AIAA

† See, for example, Landahl and Stark[36] for a general survey of lifting-surface theory as of 1968.

The position is adopted that the subject under discussion should properly include control surfaces. Special methods, akin to interference techniques, should be used for treating controls and similar devices which produce slope discontinuities and/or gaps in the geometry of planar or nonplanar lifting systems. One particular question, which has not yet been thoroughly studied, involves theoretical description of the situation where the gap between a pair of coplanar surfaces is gradually increased or decreased, as might be caused by varying the sweep angle of a wing which, in its full aft position, meshes with a fixed stabilizer. What is the size of gap at which the "inner solution" described in the next section can no longer accurately be employed, where the system must begin to be analyzed as a pair of interfering surfaces?

The present paper is concerned with three, rather distinct subjects. The first involves an attempt to identify singularities and other unique local behavior of the aerodynamic loading at edges, corners, and other irregular geometrical configurations that may be encountered on both planar and nonplanar systems. The inspiration for this undertaking derives from Landahl's paper,[1] wherein he 1) re-examined leading, side, and trailing-edge singularities and 2) presented new information on the logarithmic behavior of loading at a control-surface slope discontinuity. It is emphasized, however, that many of the results given below are speculative and that several have not yet been integrated into over-all loading methods. Some constitute valid "inner asymptotic expansions" (Van Dyke[2]), which can be matched or otherwise harmonized with

Table 1 Local singularity solutions for oscillating lifting surfaces.[a] Note that in all cases the control surface angle is $\delta(y,t) = \bar{\delta}(y)e^{-i\omega t}$

Problem	Sketch	Inner Solution for Subsonic Edge	Inner Solution for Supersonic Edge	References
Control Surface Leading Edge (No Gap or Aerodynamic Balance)	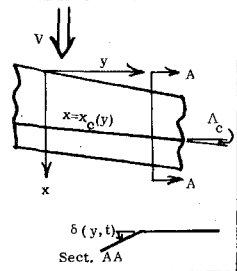	$\Delta\bar{C}_p(x,y) = \frac{-4\bar{\delta}(y)\cos\Lambda_c}{\pi\sqrt{1-M^2\cos^2\Lambda_c}} \ell n\lvert x-x_c\rvert$	No Singularity	1,5*,6*
Control Surface Side Edge	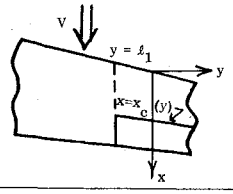	$\Delta\bar{C}_p(x,y) = \frac{4\bar{\delta}(\ell_1)}{\pi}\left\{2i\frac{\omega}{V} - \frac{\omega^2}{V^2}[x-x_c(\ell_1)]\right\}[y-\ell_1]\ell n\lvert y-\ell_1\rvert$	Apparently the Same	1,5*,6*
Control Surface Corner	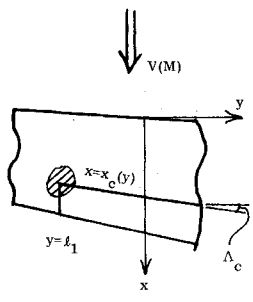	$\Delta\bar{C}_p(x,y) = \frac{-2\bar{\delta}(y)\cos\Lambda_c}{\pi\sqrt{1-M^2\cos^2\Lambda_c}} \cdot \left\{1 + 2i\frac{\omega}{V}[x-x_c(y)]\right\} \cdot \ell n\left[\sqrt{(x-x_c)^2+\beta^2(y-\ell_1)^2} - \beta(y-\ell_1)\right] + \frac{2\bar{\delta}(\ell_1)}{\pi}\left\{2i\frac{\omega}{V} - \frac{\omega^2}{V^2}[x-x_c(\ell_1)]\right\} \cdot [y-\ell_1]\ell n\left[\sqrt{(x-x_c)^2+\beta^2(y-\ell_1)^2} - (x-x_c)\right]$	Not Known to Author	1,5*,6*
Control Surface which Intersects Wingtip	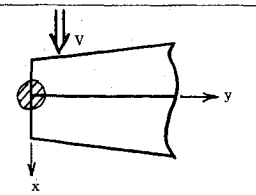	$\Delta\bar{C}_p(x,y) = \frac{-2\bar{\delta}(0)}{\pi\beta} \ell n\left[\frac{1-\sqrt{1-e^{-2Q_o}}}{1+\sqrt{1-e^{-2Q_o}}}\right]$, where $Q_o = \sinh^{-1}\left(\frac{\beta y}{\lvert x\rvert}\right)$ and $y \geq 0$ (Available for swept edge as an integral, Ref. 6)	No Singularity. Can be obtained as standard steady supersonic control surface solution (e.g., Ref. 7).	1,6

[a] Asterisks on references indicate that details are given for integrating the inner solution into general subsonic lifting surface theory.

the field in which they are imbedded; others are merely "local solutions" which may not permit such integration. One purpose in presenting these tabulations is to stimulate research into which of these situations are essentially important and thus require attention during the mechanization of computer programs for practical application.

A second aim of the paper is briefly to describe some recent activity in the United States on the analysis of interfering systems. Some unpublished calculations by Andrew's method[8] on the T-tail in subsonic flow are compared with European results. A brief account is given of a supersonic program under development at The Boeing Company, whose object is nonintersecting but noncoplanar (and possibly nonparallel) pairs of lifting surfaces. Since this method continues to rely on source-sheet elements in the form of a rectangle with diagonals parallel to the Mach lines, it is recommended that future study be given to an element in the form of a trapezium, which should improve convergence by achieving much better representations of the planform shapes of wings and tails.

Finally certain nonlinear effects are examined which are felt to have greater significance for interference problems than for isolated surfaces.

II. Categorization of Singularities and Other Local Effects

In what follows, the conventional notation of linearized, oscillatory aerodynamic theory is used wherever possible. Thus x,y,z are Cartesian coordinates, with x universally parallel to the unperturbed stream of speed V, and z normal to the x-y plane of any planar lifting surface. The perturbation velocity potential is $\varphi(x,y,z,t)$. C_p is the dimensionless perturbation pressure (acceleration potential), while ΔC_p represents the dimensionless airload per unit area exerted on a thin surface in the direction of its positive normal (e.g., z). A superscript bar denotes the complex amplitude of a simple harmonic quantity

$$\varphi(x,y,z,t) = \bar{\varphi}(x,y,z)e^{i\omega t} \tag{1}$$

with t time and ω the circular frequency.

In most, but not all, cases it is convenient to think of each independent and dependent variable as having been nondimensionalized by reference to V and some convenient chordwise wing dimension l. It is then well known that φ, C_p, or any of the perturbation velocity components u,v,w must

Table 2 Global singularities and situations where the local flow may be irregular on interfering surfaces

Problem	Sketch	Inner or Local Solution for Subsonic Edges	Supersonic Edges	References
Leading, side and Trailing Edges	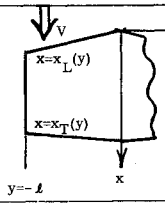	$\Delta\bar{C}_p(x,y)$ $= \begin{cases} C_1(y)[x-x_L]^{-1/2}, & \text{L. E.} \\ C_2(x)[y+\ell]^{1/2}, & \text{side edge} \\ C_3(y)[x_T-x]^{1/2}, & \text{T. E.} \end{cases}$	No Singularity	Well-Known (e.g., 1)
Swept-Wing Vertex	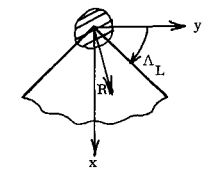	$\bar{\varphi} \sim R^n f(\frac{x}{R}, \frac{y}{R}, \frac{z}{R})$, where $n = n(\Lambda_L)$. $n \to [\frac{1}{2} + \frac{\sin\Lambda_L}{\pi}]$, $\Lambda_L \to 0$, $n \to [1 - \frac{1}{4}(\frac{\pi}{2} - \Lambda_L)^2]$, $\Lambda_L \to \frac{\pi}{2}$ $\Delta\bar{C}_p(x,y)$, in all cases, has square-root singularity at L. E.	Nonsingular Conical Flow	10 and Refs. contained therein
Other Planform Discontinuities	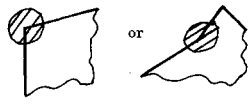	Not Know to Author	Not Known to Author	
Fold or Dihedral Change	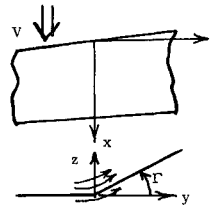	Upper surface: $\bar{\varphi}(x,y,z)$ $= C_U(x)\mathrm{Re}\left\{e^{-i[\Gamma'/(1-\frac{\Gamma}{\pi})]}(y+iz)^{\frac{\pi}{\pi-\Gamma}}\right\}$ Lower Surface: $\bar{\varphi}(x,y,z)$ $= C_L(x)\mathrm{Re}\left\{e^{i[\Gamma'/(1+\frac{\Gamma}{\pi})]}(y+iz)^{\frac{\pi}{\pi+\Gamma}}\right\}$ (Velocity singular at lower-surface corner).	Rodemich solution applies (Refs. 11, 12): Local source strength ~ (Distance from Fold Line)$^{-1}$	For Subsonic "crossflow," p. 150 of Ref. 13.
Intersection of Two Surfaces	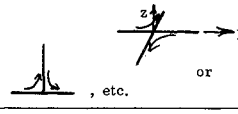	Above solution believed to apply locally. (No velocity Singularity).	Not Known to author. Rodemich method can be applied in numerical solutions.	
Gap in Wing Surface or Between Wing and Control Surface	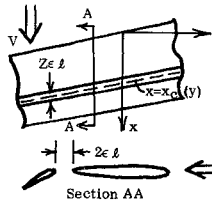	For $M \cong 0$, $u \sim i\omega$ $= C_4(y)\left\{1 - \frac{2}{\pi}\ell n\left[\frac{\eta+1+\sqrt{\eta^2-1}}{\eta+1-\sqrt{\eta^2-1}}\right]\right\}$ $+C_5(y)\sqrt{\frac{\eta+1}{\eta-1}}$, where $\eta = \frac{x-x_c(y)+iz}{\epsilon}$ C_4 and C_5 to be found by matching and Kutta condition at front edge of gap.	Not Known to Author	14 (also treats gaps parallel to the flight direction).

satisfy the acoustic equation

$$\beta^2\varphi_{xx} + \varphi_{yy} + \varphi_{zz} - M^2[ik\varphi_x - k^2\varphi] = 0 \qquad (2)$$

Here M is flight Mach number, $\beta^2 = 1 - M^2$, and $k \equiv \omega l/V$ is a dimensionless frequency.

During the analysis of singularities along particular lines on the wing planform, the origin of coordinates is often placed at a suitable point on such a line. The sketches in Tables 1 and 2 identify these locations for the cases studied. The essence of the method is then to seek the singular character of an inner expansion of the flowfield near the line. This is done[1,2] by defining the proper coordinates to be "expanded" in the inner field by division with a small quantity ϵ which measures the size of this field. Corresponding expansion in ϵ of the chosen dependent variable leads to simplified differential equations for the lowest-order terms and sometimes to elementary inner solutions, as illustrated below. Those cases are identified and referenced for which procedures have already been proposed for incorporating the inner results into over-all lifting-surface loading theories.

A. Local Singularities

The term "local singularity" is coined to denote situations where not only the form but also the strength are fixed by conditions at the singularity line, apparently independent of the general shape and motion of the lifting surface. Although well known for subsonic airfoils in two dimensions, this possibility seems to have been first published by Landahl[1] for three-dimensional control surfaces.

In order to save space, Table 1 has been constructed to summarize key information and references for those cases that are known to the author to have been studied in some detail. Table 1 is intended to be self-explanatory, with the qualification that it simply telegraphs results which are presented in extenso by the cited references. For instance, both Refs. 5 and 6 describe how the leading-edge, side-edge and corner solutions can be combined into composite formulas for $\Delta\bar{C}_p(x,y)$ appropriate to an arbitrary arrangement of trailing-edge controls and flaps performing prescribed oscillations. This formulation also accounts for the known behavior of $\Delta\bar{C}_p$ at all outer boundary edges of a single, planar lifting surface.

Preliminary applications like those of Berman, Skyprykevich, Smedfjeld, and Kelly[8] have already demonstrated the advantages of properly including certain of the control-surface singularities in general airload theories. It is expected, however, that even greater efficiency and accuracy will result from a current project of Rowe and collaborators, who are programing the problem in a manner very close to that recommended by Ref. 6.

B. Global Singularities

In contrast to the rather few situations, involving control surface edges, where the loading singularity is locally determined, the majority of cases studied here are "global" in the sense that the entire wing planform shape and upwash distribution due to the motion must be specified before the numerical coefficient of the singularity (or slope singularity) can be calculated. In those instances where the method of inner and outer expansions has been shown to apply, this coefficient is fixed by the "matching" process. Landahl[1] used this approach to study the familiar loading behavior near leading and side edges; it is believed that matching might be employed on this problem. Conventional three-dimensional subsonic procedures of the Multhopp and Watkins type, however, simply include the singular edge terms in the assumed pressure loading functions and therefore converge on what amounts to an outer solution (cf. the discussion of potential theory for lifting surfaces in Ref. 9).

Table 2 again tries to summarize key information and references, where available, on the majority of configurations where some sort of irregular behavior of the local flow is likely to have to be accounted for. Wherever undetermined coefficients in forms like $C_i(x)$, $C_j(y)$ appear in the table, it is understood that their values depend on the global flow pattern. No implication is intended that the manner of their determination is known in all cases. But for the gap in the wing planform, White and Landahl[14] furnished some ingenious examples of matching which appear capable of extension to unsteady flow and to other geometries in this case.

The appearance of undetermined coefficients reflects the fact that the lowest-order inner expansions of the solutions in Table 2 are actually eigenvalue problems, with entirely homogeneous boundary conditions. By way of illustration, one might outline Landahl's approach[1] to the leading-edge singularity. As dependent variable, he chooses the pressure-coefficient amplitude $\bar{C}_p(x,y,z)$, which also must satisfy Eq. (2). The principal boundary conditions are that

$$\bar{C}_p(x,y,o) = 0 \tag{3}$$

ahead of the leading edge $x = x_L(y)$, whereas $\partial\bar{C}_p/\partial z$, which is proportional to the vertical component of fluid particle acceleration, must be a "regular function" of x,y for $x > x_L(y)$. Now inner variables

$$\bar{x} \equiv (x - x_L)/\epsilon, \quad \bar{z} \equiv \bar{z}/\epsilon \tag{4}$$

are chosen to focus attention on a small volume of linear dimension ϵ centered along the edge, and $\bar{C}_p$ is subjected to an inner expansion

$$\bar{C}_p(\bar{x},y,\bar{z}) = \sum_{n=0} \epsilon^n \bar{C}_p{}^{(n)}(\bar{x},y,\bar{z}) \tag{5}$$

The various orders in ϵ of the exact problem statement are then separately equated. $\bar{C}_p{}^{(0)}$ is found to be governed by a quasi-steady equation (typical of all these cases)

$$[(1 - M^2\cos^2\Lambda_L)/\cos^2\Lambda_L]\bar{C}_{p_{\bar{x}\bar{x}}}{}^{(0)} + \bar{C}_{p_{\bar{z}\bar{z}}}{}^{(0)} = 0 \tag{6}$$

where Λ_L is the local sweep angle. Because $(\partial/\partial z) = \epsilon^{-1} \times (\partial/\partial\bar{z})$, the right-hand side of the boundary condition on the wing vanishes, leaving

$$\bar{C}_{p_{\bar{z}}}{}^{(0)}(\bar{x},y,o) = 0, \quad \bar{x} > 0 \tag{7}$$

and, as above

$$\bar{C}_p{}^{(0)}(x,y,o) = 0, \quad \bar{x} < 0 \tag{8}$$

Since Eq. (6) is essentially a Laplace equation, a general eigensolution of the form

$$\bar{C}_p{}^{(0)}(\bar{x},y,\bar{z}) = C_1(y)Re\left\{\left[\bar{x} + i\frac{(1 - M^2\cos^2\Lambda_L)^{1/2}}{\cos\Lambda_L}\bar{z}\right]^{m-1/2}\right\} \tag{9}$$

can readily be constructed. From physical considerations, one reasons that the integer m should be 0 for a leading edge. Since $m = 1$ applies to trailing and side edges, a variety of important results can be recovered from this single exercise after minor adjustments in the chosen independent variables.

A somewhat different result from Eq. (9) was given by Küssner[4] but has since been revised by him. In a very stimulating presentation to the conference mentioned in the title footnote, Küssner also verified Landahl's singularity for the control surface, starting from the fundamental Green's function of wing theory.

As a second illustration, consider the vertex of a swept or delta lifting surface pictured in Table 2. The relationship of this problem to the one actually analyzed by Brown and Stewartson[10] can be explained by working with $\varphi(x,y,z)$ as the basic quantity describing the flowfield. The exact $\bar{\varphi}$ must satisfy Eq. (2), together with the familiar conditions near the vertex

$$\bar{\varphi}(x,y,o) = 0, \text{ (ahead of L.E.)} \tag{10}$$

and

$$\bar{\varphi}_z(x,y,o) = \text{Specified regular } f(x,y), \text{ (behind L.E.)} \tag{11}$$

In the inner region there is no preferred independent variable, so all are expanded by division with the inner dimension ϵ

$$\bar{x},\bar{y},\bar{z} = x,y,z/\epsilon \tag{12}$$

The lowest-order term in an expansion similar to Eq. (5) is then obviously governed by

$$\beta^2\bar{\varphi}_{\bar{x}\bar{x}}{}^{(0)} + \bar{\varphi}_{\bar{y}\bar{y}}{}^{(0)} + \bar{\varphi}_{\bar{z}\bar{z}}{}^{(0)} = 0 \tag{13}$$

$$\bar{\varphi}_{\bar{z}}{}^{(0)}(\bar{x},\bar{y},o) = 0, \quad |\theta| \leq (\pi/2 - \Lambda_L) \tag{14}$$

$$\bar{\varphi}^{(0)}(\bar{x},\bar{y},o) = 0, \quad (\pi/2 - \Lambda_L) < \theta < (3\pi/2 + \Lambda_L) \tag{15}$$

where θ is a polar angle measured counterclockwise from the x axis. One final step is to use the familiar Prandtl-Glauert transformation to convert Eq. (13) into Laplace's equation

$$\Delta^2\bar{\varphi}^{(0)} = 0 \tag{16}$$

The boundary conditions are unaltered except for a change in the leading-edge swept angle through

$$\tan\Lambda_{L_1} = (1/\beta)\tan\Lambda_L \tag{17}$$

Brown and Stewartson[10] furnish a very complete solution of this inner problem based on the assumption

$$\bar{\varphi}^{(0)}(\bar{x},\bar{y},\bar{z}) = \bar{R}^n f(\bar{x}/\bar{R}, \quad \bar{y}/\bar{R}, \quad \bar{z}/\bar{R}) \tag{18}$$

where $\bar{R} = (\bar{x}^2 + \bar{y}^2 + \bar{z}^2)^{1/2}$. Specifically, f is replaced by a series of separated products $G(\sigma)H(\nu)$, where σ and ν are homogeneous variables having constant values in the $\bar{z} = 0$ plane on and off the wing, respectively. The exponent n is found to vary from $\frac{1}{2}$ to 1 as Λ_{L_1} increases from 0 (straight wing) to $\pi/2$ (low-aspect ratio delta). Careful examination of the corresponding loading $\Delta\bar{C}_p(x,y)$ proves it always to be singular as the inverse square-root of distance from the leading edge as that edge is approached, but the inner solution provides no information on the coefficient of the singularity.

It must be admitted that no way seems to have been found to "match" the Ref. 10 results to over-all load distributions for swept surfaces. Indeed, it is a "local solution" in the

Table 3 Generalized forces on an oscillating T-tail

$k = 0.21$		$M = 0.376$	
Source	$C_{y,\psi}$	$C'_{l,\psi}$	$C'_{n,\psi}$
Experiment[17]	$1.306e^{i(-1°)}$	$-1.81e^{i\cdot(3°)}$	$0.616e^{i(-1°)}$
Davies[18]	$1.16e^{i\cdot(12°)}$	$-1.914e^{i\cdot(12°)}$	$0.621e^{i(-11°)}$
Andrew[3]	$1.320e^{i\cdot(3°)}$	$-2.126e^{i\cdot(5°)}$	$0.730e^{i(-4°)}$

sense of Van Dyke[2] and, like the wing-fold solution and others in Table 2, does not behave in a physically reasonable manner at long distances from the vertex. It can also be proved that the region of the planform within which it significantly affects the flow is exponentially small. The question as to when it may be sufficiently important to be included in practical programs has yet to be answered. One cause of uncertainty is early experience with discrete-element (Falkner) calculations of the loading on swept wings, where it sometimes proved necessary to insert special terms to account for conditions at pointed vertices.

III. Recent Developments Relative to Interfering Systems

In a recent survey Mykytow[15] summarized the results of several investigations on subsonic and supersonic interfering surfaces which were in progress in the United States. Subsequently there have occurred a few calculations and program refinements which the author wishes to describe here.

First, some subsonic generalized forces are given which were recently computed for T-tails by Andrew.[3] Andrew's theory is essentially an adaptation of the method of Laschka[16] to sets of intersecting planar surfaces. Although the details are not reviewed here, the three singularities of the well-known kernel function are isolated, and extreme care is taken with integrations of the products of each of these with the various terms in a Chebyshev-polynomial series for the load distribution. Since there have been some past difficulties with the demanding task of programing, these results must still be regarded as preliminary. The theory itself is so highly refined, however, that their presentation is believed to be justified.

Table 3 lists generalized forces due to yawing oscillation for the T-tail tested by Clevenson and Leadbetter,[17] which consisted of a rectangular horizontal mounted at the top of a rectangular vertical, of equal chord, and rotated about a vertical axis at 50% of the chord. In the notation of Ref. 17, calculations by Andrew and Davies[18] are compared with test results for the following dimensionless quantities: side force, rolling moment about an axis below the base of the model, and yawing moment about the axis of yaw. Each is given in amplitude and phase-angle form, and the reduced frequency $k = 0.21$ is based on full chord.

Figure 3 depicts the T-tail originally analyzed by Stark[19] for oscillations in yaw, lateral translation and roll. Theoretical generalized forces computed by five different theories are tabulated, in standardized nondimensional notation. Information on k, M, etc., is listed in the figure. Since the sources of these various calculations were identified in Ref. 15, from whose Fig. 1 the present format was adapted, there is no need to repeat them here. Each of the Andrew calculations is based on an assumed pressure series which included three terms chordwise and four terms spanwise (accounting for antisymmetry in the loading of the horizontal) for each of the two lifting elements.

The agreement among the results in Table 3 is believed to be as good as can be expected at the present state of development. There is more variability shown in Fig. 1, with several of the numbers given by Andrew falling outside any reasonable "scatter band" based on the mean deviation of the corresponding numbers from the other four sources. It is recommended that further study be devoted to the status of

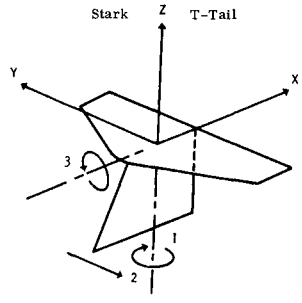

		Yaw		Side Translation		Roll	
		Re	Im	Re	Im	Re	Im
Davies [Ref. 18]		-0.0846	-0.5090	0.0461	-0.0283	0.0141	0.0260
Stark [Ref. 19]		-0.0961	-0.4811	0.0412	-0.0300	0.0125	0.0239
NLR	Yaw	-0.0922	-0.5155	0.0466	-0.0298	0.0145	0.0259
MDC		-0.0837	-0.5270	0.0470	-0.0278	0.0137	0.0257
Andrew [Ref. 3]		-0.1486	-0.3960	0.0277	-0.0376	0.0204	0.0253
Davies		-0.6224	-0.3754	0.0265	-0.1234	0.0169	-0.0305
Stark	Side	-0.6108	-0.3625	0.0241	-0.1211	0.0158	-0.0295
NLR	Trans-	-0.6236	-0.3728	0.0260	-0.1236	0.0168	-0.0304
MDC	lation	-0.6270	-0.3965	0.0297	-0.1260	0.0171	-0.0318
Andrew		-0.5820	-0.3877	0.0355	-0.1248	0.0285	-0.0285
Davies		-0.1248	-0.1237	0.0150	-0.0262	0.0179	-0.0502
Stark		-0.1247	-0.1151	0.0134	-0.0255	0.0179	-0.0497
NLR	Roll	-0.1235	-0.1217	0.0148	-0.0259	0.0179	-0.0502
MDC		-0.1270	-0.1266	0.0154	-0.0269	0.0186	-0.0529
Andrew		-0.2403	-0.1649	0.0169	-0.0520	0.0093	-0.0139

$M = 0.8$; $\frac{\omega s}{V} = 0.6$; (s = semispan of horizontal)

Fig. 1 Comparison of generalized aerodynamic forces for the Stark T-tail.

the convergence of Andrew's results, as by adding terms to the various pressure series and refining the network of collocation points on the horizontal and vertical surfaces.

Another recent undertaking of possible interest is the computer program being prepared by Rowe, Ii, and collaborators at The Boeing Company, under contract to U.S. Air Force Flight Dynamics Laboratory, for the purpose of finding airloads and generalized forces on oscillating wing-horizontal tail combinations by linearized supersonic theory. Both wing and tail are allowed to have finite, constant dihedral angle. The tail is influenced in the obvious way by flow perturbations due to the wing and wake, but it is assumed to be so far aft as to place the wing outside the tail's zone of influence. It would not be a major modification to a program of this sort, however, to account for the mutual interference that might occur with biplane wings.

The basis of Rowe's computational procedure is to approximate wing and tail—together with "diaphragms" to represent the wake and disturbed portions of the lifting-surface planes adjacent to any subsonic edges—by means of a pattern of uniform supersonic sources over rectangular area elements whose diagonals are parallel to the Mach lines. Thus it is just an extension of the familiar "Mach box" method.[20] This

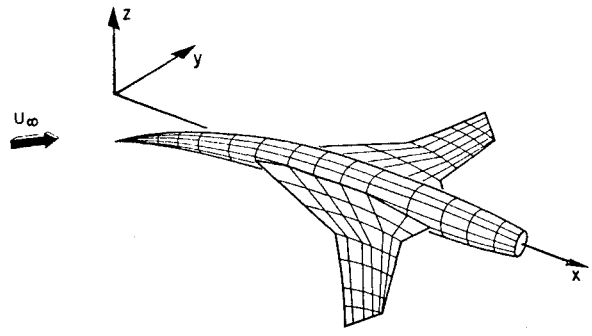

Fig. 2 Representation of a wing-fuselage combination with trapezium elements, in the manner of Ref. 22.

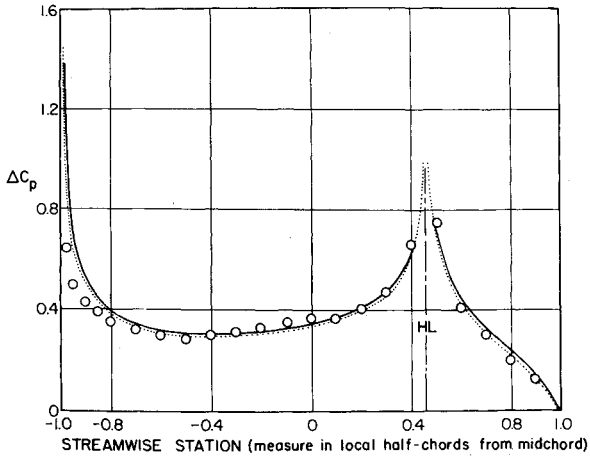

Fig. 3 Predicted chordwise load distributions on tail of Ref. 34, compared with measured data given as circles. Solid line is linearized boundary condition; dotted line uses boundary condition Eq. (20). (M = 0.21; elevator deflection 10°.)

method has, of course, been employed previously for supersonic interference problems (e.g., Donato and Huhn[23]), but there are differences from earlier programs in such respects as the manner of treating surfaces with dihedral and subdivision of the Mach-box grid (where necessary) for increasing the accuracy of the Aerodynamic Influence Coefficients (AIC's). Considerable effort has been spent in deriving efficient AIC formulas for velocity potential and for all three components of the perturbation velocity, the basic approach being that taken in Ref. 21.

No computations are yet available from this supersonic interference program. The first results are expected at about the end of the year, and it is planned later to use the program on standardized interacting configurations like those agreed upon by the AGARD Structures and Materials Panel.

In view of the now widely demonstrated effectiveness of unsteady supersonic theory as applied through the use of source sheets, diaphragms and AIC's, the author wishes to propose a small refinement, which seems the next logical step toward improving numerical accuracy. The suggestion is to adopt an area element in the form of a trapezium,‡ with two sides parallel to the flight direction and the others swept back at arbitrary angles. This element forms the building block for the extensive work by Woodward and collaborators[22] on wings and wing-body combinations in steady flow, both subsonic and supersonic. Figure 2, adapted from one of Woodward's illustrations, shows the precision with which a typical aircraft layout can be matched when small planar elements of this sort are used. One can compare this picture with the jagged, "stair step" arrangement of Mach boxes that would be needed to approximate the various swept edges. As long as the lifting-surface planform is bounded by straight lines, a very precise representation will usually be possible. The principal anticipated difficulty, and one which must be investigated further, will occur with such situations as the diaphragm region ahead of a subsonic leading edge near the vertex of a swept wing.

The main obstacle to mechanizing an oscillatory Woodward program would seem to be in the development of formulas for the necessary AIC's which cover all possible combinations of Mach number and edge sweep. This proved to be a nontrival undertaking even in steady flow, as evidenced by the many exasperating misprints in Ref. 22. The Appendix discusses this mathematical problem in more detail and presents what are believed to be efficient formulas for the $\bar{u},\bar{v},\bar{w}$ and $\bar{\varphi}$ AIC's in one particular case. No inference should be drawn, however, that the matter of finding the best AIC expressions for all purposes has been settled, so that the only remaining job is merely to mechanize airload computations. Indeed, the Woodward element has been criticized on the grounds of requiring an unusual choice of downwash collocation point and of being sensitive to this choice. The addition of unsteadiness may exacerbate this difficulty. On the other hand, there is a great advantage in being able to adopt various geometrical and surface-fitting routines that have already been perfected for use in steady flow.

While on the subject of the trapezium area element, it is worth mentioning that this same shape has proved useful in the development of a vortex-lattice subsonic theory for oscillating, coplanar wing-tail configurations (Albano[24] based on the method of Rodden and Albano[25]). This procedure is typical of several similar lattice applications carried out recently in the U.S. and elsewhere on planar wings, wing-body combinations and interfering systems. The idea of the vortex lattice is not new but has a long history extending back to generalized lifting-line and Falkner[26] methods prior to and during World War II. For subsonic unsteady flow, a double lifting-line scheme was employed by Goland et al.[27] as early as 1954; W. P. Jones proposed and applied a procedure[28] which also contains elements of a lattice method for upwash computation.

The success of this approach is not believed, however, to provide a justification for the abandonment of attempts to improve continuous solutions of the integral equation. The latter alternative offers the possibility of exact treatment of local singularities like those discussed in Sec. II.

IV. Thickness, Boundary-Layer, and Wake Effects

Landahl and the present author, writing in the AGARD Manual on Aeroelasticity,[29] recently undertook a comprehensive review of efforts to introduce nonlinearity into unsteady airload solutions. With the exceptions of the hypersonic flow regime and of two-dimensional airfoils, the available products are somewhat disappointing. That is to say, either an enormous computational effort is required to obtain results of limited applicability or, in some cases, numerical applications have proved unfeasible. Without any denigration of the impressive contributions contained in their work, these difficulties are typified by the investigations of Djojodihardjo and Widnall,[30] Andrew and Stenton,[31] and Kacprzynski et al.,[32] for incompressible, transonic, and supersonic flow, respectively. It is urged that attempts to mechanize these theories be continued.

But while aeroelasticians wait for the realization of such hopes, there remains a near-term need for simpler engineering means of accounting for important nonlinearities. Without claiming originality, the author wishes to call attention here to two such "irrational correction methods" which surely deserve more thorough study then they have received in the past. The first would seem to have special value in predicting more accurate loads on trailing-edge control surfaces, the second on interfering wing-tail systems.

As a means of refining aerodynamic theory for lifting surfaces, it has often been suggested that the conventional linearized field differential equations might be combined with a nonlinear statement of the kinematic boundary condition and/or with a nonlinear pressure-velocity relation. It is well-known that this combination represents a rational approximation for slender bodies of revolution, and schemes for applying it to steady airfoil flow go back at least as far as Allen's.[33] There is also partial justification for the ad hoc method proposed below in the idea of "local linearization" (cf. discussion on pp. 20–23 of Ref. 29).

On a three-dimensional wing of moderate to large aspect ratio, the upwash velocity for use in solving the linearized

‡ For a promising alternative proposal, involving the general triangular element, see Kariappa and Smith.[37]

integral equation is normally computed from the known mean-surface motion $z_a(x,y,t)$ by the formula

$$w(x,y,o,t) = \frac{1}{V}\frac{Dz_a}{Dt} = \frac{1}{V}\left[\frac{\partial z_a}{\partial t} + \frac{\partial z_a}{\partial x}\frac{\partial x}{\partial t}\right] \quad (19)$$

where $\partial x/\partial t$ is equated to the freestream speed V. All wings have finite thickness, however, and no complication arises if $\partial x/\partial t$ is replaced by a local velocity $V_L(x,y)$ at the wing surface due to the combined steady-state effects of this thickness and boundary layer displacement. The (dimensionless) upwash would then become

$$w(x,y,o,t) = (1/V)[\partial z_a/\partial t + V_L(x,y)(\partial z_a/\partial x)] \quad (20)$$

at both upper and lower surfaces, $V_L(x,y)$ can be estimated from theory or, preferably, computed from wind-tunnel measurements of the pressure distribution due to thickness. The greater inconvenience of introducing unsteady boundary-layer effects in Eq. (20) is discussed in Sec. 4.2 of Ref. 29, where it is shown that the condition $k \ll 1$ on reduced frequency suffices for the boundary layer to be treated as quasi-steady.

Given a sinusoidal $w(x,y,o,t)$, linearized (subsonic or supersonic) potential theory is capable of furnishing information on $\bar{\varphi}$ and all perturbation velocity components of the wing surface. Without rational justification, one can then give consideration to the use of a second-order Bernoulli equation [cf. Eq. (4) of Ref. 29]

$$C_p = -2[\varphi_x + \varphi_t] + M^2[\varphi_x + \varphi_t]^2 - [\varphi_x^2 + \varphi_y^2 + \varphi_z^2] \quad (21)$$

Here φ denotes the entire perturbation potential, with local effects due to thickness included. When simple harmonic motion is assumed, about a mean condition of thickness flow at zero incidence, this relationship simplifies if adapted to the computation of lifting pressure difference $\Delta\bar{C}_p(x,y)e^{ikt}$

$$\Delta\bar{C}_p(x,y) \cong 4\{\bar{u}(x,y,o+) + ik\bar{\varphi}(x,y,o+) - 4M^2V_L(x,y)[\bar{u}(x,y,o+) + ik\bar{\varphi}(x,y,o+)] + 4V_L(x,y)\bar{u}(x,y,o+)\} \quad (22)$$

Here the effect of thickness in inducing spanwise and normal velocity components has been neglected. But even if these small refinements are added, the computational difficulty of going to Eq. (22) is trivial by comparison with the numerical solution of the flowfield problem.

In Ref. 6, a recent example was given of the consequences of adopting only the correction Eq. (20) when calculating steady loading due to a deflected flap. This was a full-span elevator tested by Tinling and Dickson.[34] Figures 3 and 4 summarize two cases of comparison between lifting pressure differences and the uncorrected and corrected predictions. Sensible improvement is obtained for the loading on the flap (although the differences are not large).

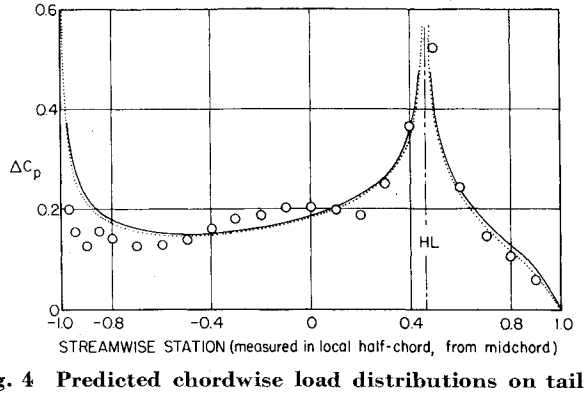

Fig. 4 Predicted chordwise load distributions on tail of Ref. 34, compared with measured data given as circles. Solid line is linearized boundary condition; dotted line uses boundary condition Eq. (20). (M = 0.80; elevator deflection 4°.)

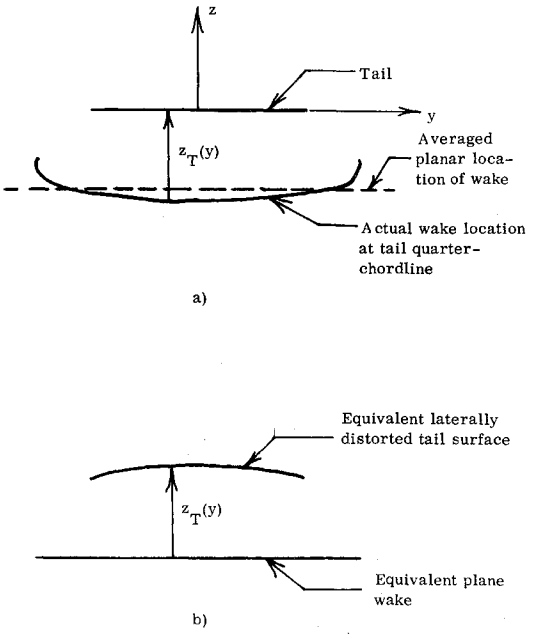

Fig. 5 Rear views of a planar horizontal tail surface with the steady-state wing wakes as it passes the tail quarter-chordline. In a is shown an average planar wake surface that might be used with current interference programs. In b, the wake is arbitrarily flattered, so that its vortex sheet can be easily related to that of the wing ahead, while the tail is curved into a nonplanar surface which preserves vertical separation $z_T(y)$ at each spanwise station.

The author's second proposal concerns the manner of positioning the wake of the wing, as it passes the tail, when calculating interference on a conventional tailed configuration. Present programs (cf. the examples described and cited in Ref. 15) either require coplanar orientation, assume that the wake propagates aft in the freestream direction or, at the most, retain a planar wake which is positioned relative to the aft surface at a vertical separation determined from the trimmed flight condition. Such approximations may apply for, say, flutter analysis of a very closed-coupled wing and tail, but more generally they can be improved upon.

Any free or forced sinusoidal oscillation of a flying airplane structure constitutes a relatively small perturbation upon its state of equilibrium flight. The oscillatory portion of the vortex sheet from the wing trailing edge is therefore rather weak and it seems reasonable, on the average, to assume that the entire wake follows the steady trailers quite closely. From wind-tunnel tests or flight measurements, one knows the downward and outward wake displacement relative to the wing plane and the curling up of its edges. For wing-tail interference calculations where there is significant fore-aft separation, it is suggested that the nonlinear influence of the steady flowfield be introduced by locating the oscillatory wake surface in accordance with the best available steady data. In this fashion, the effects of flight altitude, path angle, wing loading and similar parameters on wing-tail flutter behavior can be accounted for through wholly linearized aerodynamic methods.

There appear to be two levels of sophistication at which the proposed adjustment can be introduced. The simplest would be adaptable to interference programs where both lifting surfaces are taken to be planar, although not lying in the same plane. Here some average, planar position must be assigned to the (laterally distorted) wake, perhaps by averaging the vertical separation across the tail span along its quarter-chord line. An improvement can be imagined for use with programs, like Rowe's just described, which account for nonplanar mean surfaces of both wing and tail. Clearly,

means will have to be found for representing both the downward and outward displacements of the shed vortex sheet induced by the steady wake distortion. In actuality, the easiest scheme might be arbitrarily to distort the lateral shape of the tail while keeping the wake in a single plane, as illustrated in Fig. 5b. Figure 5 has been prepared to summarize the entire scheme.

Appendix: Aerodynamic Influence Coefficients for the Trapezium Area Element in Oscillatory Supersonic Flow

Figure 6a depicts the trapezium area element which forms the building block of Woodward's[22] various methods for subsonic and supersonic airload prediction on interfering systems. This Appendix treats only the problem of adapting this element to the analysis of aggregates of oscillating supersonic lifting surfaces by means of sources and AIC's. The process of replacing each lifting surface in this system, together with the diaphragms needed for isolating its upper and lower sides, is an obvious extension of rectangular-element schemes described in places like Refs. 20, 21, and 35. This subject is therefore skipped here, and attention is turned at once to the derivation of AIC formulas, which proves to be a task requiring considerable care.

With constant-strength oscillatory supersonic sources distributed over area S, one requires in general the potential amplitude $\bar{\varphi}$ and the velocities $\bar{u},\bar{v},\bar{w}$ at an arbitrary field point x,y,z. If these quantities are available for sources on the area shown in Fig. 6b, however, it is an easy matter to superimpose the results (Fig. 6c) to obtain them for area S. Thus if $\bar{\varphi}(x,y,z)$ represents the basic potential, then the potential for S is

$$\bar{\varphi}_S(x,y,z) = \bar{\varphi}(x - x_1, y - y_1, z) - \bar{\varphi}(x - x_2, y - y_2, z) - \bar{\varphi}(x - x_3, y - y_3, z) + \bar{\varphi}(x - x_4, y - y_4, z) \quad \text{(A1)}$$

The reader will have no difficulty writing expressions for x_i,y_i by reference to the figure.

It is well known that a unit oscillatory source sheet over any area S is characterized by the potential

$$\bar{\varphi}(x,y,z) = -\frac{1}{\pi} Re \left\{ \iint_S \frac{e^{-i\bar{k}(x-\xi)} \left[\cos\left[(\bar{k}/M)\{(x-\xi)^2 - \beta^2[(y-\eta)^2 + z^2]\}^{1/2}\right]\right]}{\{(x-\xi)^2 - \beta^2[(y-\eta)^2 + z^2]\}^{1/2}} d\xi d\eta \right\} \quad \text{(A2)}$$

Here the independent variables have been nondimensionalized, and

$$\bar{k} = kM^2/\beta^2 \equiv kM^2/(M^2 - 1) \quad \text{(A3)}$$

For practical evaluation of (A2) and its derivatives with respect to x, y, and z, the operation of taking the real part must be replaced by an actual specification of limits. These depend on what portions of S can influence the field at (x,y,z). For instance, if S is the triangular area in Fig. 6b and (x,y,z) so located that its forward Mach cone intersects the source sheet on the hyperbola illustrated there, one finds

$$Re\left\{\iint (\ldots) d\xi d\eta\right\} = \int_0^{\eta_0} \int^{x-\beta[(y-\eta)^2+z^2]^{1/2} \equiv \zeta_0} (\ldots) d\xi d\eta \quad \text{(A4)}$$

To facilitate this specification of limits in the several cases which can arise, the "decision tree" in Fig. 7 has been constructed. It is remarked that this diagram may need some refinement and that the case of the exactly sonic edge, $\beta = \tan\Lambda \equiv L$, obviously requires special treatment.

As an illustration and to save space, only the case of the subsonic edge, $\beta < L$, is developed here; the "tree" then shows the immediate necessity of assuming $x > \beta(y^2 + z^2)^{1/2}$, whereupon the value of the limit η_0 is as given there. Four special integral and series formulas, generalizations of those used for the derivation of AIC formulas in Ref. 20, prove useful

$$\int_0^\infty J_0[A(\tau^2 + b^2)^{1/2}] \cos B\tau d\tau = \begin{cases} \dfrac{\cos[b(A^2 - B^2)^{1/2}]}{(A^2 - B^2)^{1/2}} & A > |B| \geq 0 \\ 0, & A < |B| \end{cases} \quad \text{(A5)}$$

$$J_0[A(\tau^2 + b^2)^{1/2}] = J_0(A\tau)J_0(Ab) + 2\sum_{r=1}^{\infty} (-1)^r J_{2r}(A\tau)J_{2r}(Ab) \quad \text{(A6)}$$

$$\int_0^\infty J_0(A\tau) \frac{\sin B\tau}{\tau} d\tau = \text{Prin}\left[\sin^{-1}\frac{B}{A}\right] \equiv \begin{cases} \sin^{-1}B/A, & A > |B| \geq 0 \\ \pi/2, & B > A > 0 \\ -\pi/2, & B < -A \end{cases} \quad \text{(A7)}$$

$$\int_0^\infty J_{2r}(A\tau) \frac{\sin B\tau}{\tau} d\tau = \frac{1}{2r} \sin\left(2r \sin^{-1}\frac{B}{A}\right) \quad A > |B| \geq 0 \quad \text{(A8)}$$

Equation (A2) is reorganized through a reversal of the order of integration and definition of new variables $\bar{\xi} \equiv x - \xi$, $\bar{\eta} \equiv y - \eta$

$$\bar{\varphi}(x,y,z) = -\frac{1}{\pi} Re \times \left\{ \int_{\beta z}^{x} e^{-ik\bar{\xi}} \int_{y-(x-\bar{\xi})/L}^{y} \frac{\cos[(\bar{k}/M)(\bar{\xi}^2 - \beta^2[\bar{\eta}^2 + z^2])^{1/2}]}{(\bar{\xi}^2 - \beta^2[\bar{\eta}^2 + z^2])^{1/2}} d\bar{\eta} d\bar{\xi} \right\} \quad \text{(A9)}$$

By means of expressions (A5)–(A8), one finds that the inner integral can be evaluated, while accounting for the operation of taking the real part, as follows:

$$Re\left\{\int_{y-(x-\bar{\xi})/L}^{y} \frac{\cos\{(\bar{k}/M)(\bar{\xi}^2 - \beta^2[\bar{\eta}^2 + z^2])^{1/2}\}}{(\bar{\xi}^2 - \beta^2[\bar{\eta}^2 + z^2])^{1/2}} d\bar{\eta}\right\} = \frac{J_0[(\bar{k}/M)(\bar{\xi}^2 - \beta^2 z^2)^{1/2}]}{\beta} \left\{\text{Prin}\left[\sin^{-1}\left(\frac{\beta y}{(\bar{\xi}^2 - \beta^2 z^2)^{1/2}}\right) - \sin^{-1}\beta\left(\frac{y - (x - \bar{\xi})/L}{(\bar{\xi}^2 - \beta^2 z^2)^{1/2}}\right)\right]\right\} + \frac{2}{\beta}\sum_{r=1}^{\infty} \frac{(-1)^r}{2r} \times J_{2r}\left[\frac{\bar{k}}{M}(\bar{\xi}^2 - \beta^2 z^2)^{1/2}\right] \left\{\text{Prin}\left[\sin\left(2r \sin^{-1}\frac{\beta y}{(\bar{\xi}^2 - \beta^2 z^2)^{1/2}}\right) - \sin\left(2r \sin^{-1}\frac{\beta[y - (x - \bar{\xi})/L]}{(\bar{\xi}^2 - \beta^2 z^2)^{1/2}}\right)\right]\right\} \quad \text{(A10)}$$

The definition of Prin[...] here should be evident from Eq. (A7). It turns out that the principal parts in the last line of Eq. (A10) vanish outside the range of variables where the magnitude of the argument of $\sin^{-1}(\ldots)$ exceeds unity. For the second of these arcsines, and when $y \geq 0$ ($y < 0$ can be handled by symmetry), this changeover occurs at the right corner of the integration area in Fig. 6b and leads to the definition of another integration limit

$$\bar{\xi}_{00} \equiv x - \eta_0/L \quad \text{(A11)}$$

where η_0 has the value given in the "decision tree."

A combination of the foregoing results produces the final version of the potential of the triangular area: when $\beta < L$,

$$\bar{\varphi}(x,y,z) = -\frac{1}{\pi} \times \left\{ \int_{\beta z}^{\beta(y^2+z^2)^{1/2}} e^{-ik\bar{\xi}} \left[\frac{\pi J_0[\bar{k}/M(\bar{\xi}^2 - \beta^2 z^2)^{1/2}]}{2\beta} \right] d\bar{\xi} + \int_{\beta(y^2+z^2)^{1/2}}^{x} \left[J_0 \left[\frac{\bar{k}}{M} (\bar{\xi}^2 - \beta^2 z^2)^{1/2} \right] \sin^{-1} \left(\frac{\beta y}{(\bar{\xi}^2 - \beta^2 z^2)^{1/2}} \right) + \frac{1}{\beta} \sum_{r=1}^{\infty} \frac{(-1)^r}{r} J_{2r} \left[\frac{\bar{k}}{M} (\bar{\xi}^2 - \beta^2 z^2)^{1/2} \right] \sin \times \left(2r \sin^{-1} \frac{\beta y}{(\bar{\xi}^2 - \beta^2 z^2)^{1/2}} \right) \right] d\bar{\xi} - \int_{\beta z}^{\bar{\xi}_{00}} e^{-ik\bar{\xi}} \times \left[\frac{\pi J_0[(\bar{k}/M)(\bar{\xi}^2 - \beta^2 z^2)^{1/2}]}{2\beta} \right] d\bar{\xi} - \int_{\bar{\xi}_{00}}^{x} \frac{e^{-ik\bar{\xi}}}{\beta} \times \left[J_0 \left[\frac{\bar{k}}{M} (\bar{\xi}^2 - \beta^2 z^2)^{1/2} \right] \sin^{-1} \left(\frac{\beta[y - (x - \bar{\xi})/L]}{(\bar{\xi}^2 - \beta^2 z^2)^{1/2}} \right) + \frac{1}{\beta} \sum_{r=1}^{\infty} \frac{(-1)^r}{r} J_{2r} \left[\frac{\bar{k}}{M} (\bar{\xi}^2 - \beta^2 z^2)^{1/2} \right] \sin \times \left(2r \sin^{-1} \frac{\beta[y - (x - \bar{\xi})/L]}{(\bar{\xi}^2 - \beta^2 z^2)^{1/2}} \right) \right] d\bar{\xi} \right\} \quad \text{(A12)}$$

There are probably some respects in which Eq. (A12) can be simplified, but a "closed form" is out of the question. The series which appear are rapidly convergent in the parameter ranges of interest, and the substantial experience available with Mach box AIC's should contribute to effective numerical evaluations. In view of the strong similarity between (A12) and the velocity potential AIC for the Mach box, no difficulty or excessive computational cost is anticipated.

When Eq. (A12) is differentiated with respect to x,y, and z, one obtains similar formulas for the three components of perturbation velocity. $\bar{v}$ and $\bar{w}$ for the trapezium box can be built up as in Eq. (A1) and are needed in connection with

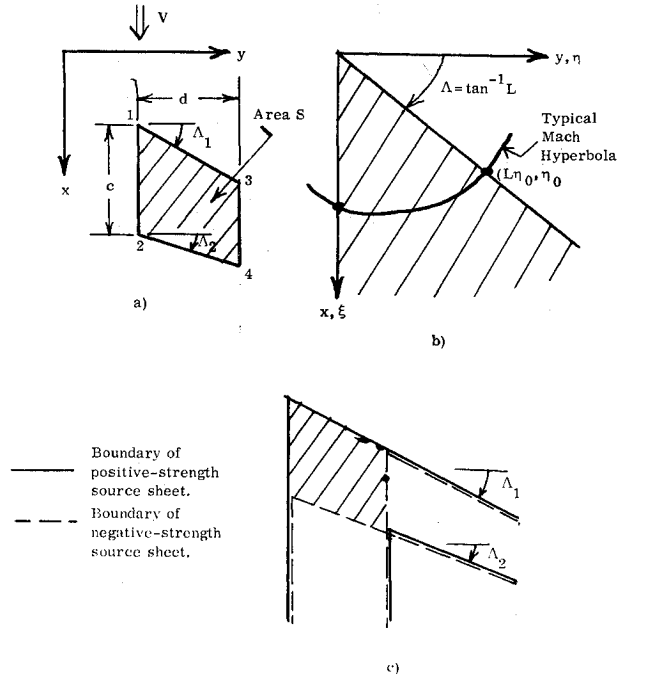

Fig. 6 a) The basic Woodward area element. b) Uniform triangular source sheet, of constant strength, extending to infinity. c) Construction of the Woodward element from four of the source sheets in b, two with unit positive strength and two with unit negative strength.

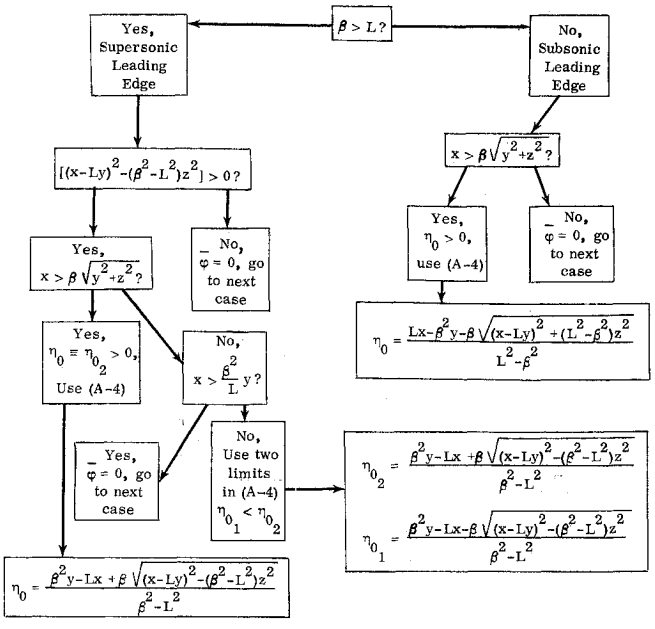

Fig. 7 Decision tree.

interference calculations between planar and nonplanar surfaces. $\bar{u}$ is also required if the details of pressure distribution (rather than weighted integrals thereof) must be determined. The expression for $\bar{w}(x,y,z)$ is too long to warrant its reproduction here, but the other two components read as follows:

$$\bar{u}(x,y,z) = -\frac{1}{\pi} \int_{\bar{\xi}_{00}}^{x} \times \frac{e^{-ik\bar{\xi}}}{\{(L^2 - \beta^2)\bar{\xi}^2 + 2\beta^2(x - Ly)\bar{\xi} - \beta^2[(x - Ly)^2 + L^2 z^2]\}^{1/2}} \times \left\{ J_0 \left[\frac{\bar{k}}{M} (\bar{\xi}^2 - \beta^2 z^2)^{1/2} \right] + 2 \sum_{r=1}^{\infty} (-1)^r J_{2r} \left[\frac{\bar{k}}{M} \times (\bar{\xi}^2 - \beta^2 z^2)^{1/2} \right] \cos \left(2r \sin^{-1} \frac{\beta[y - (x - \bar{\xi})/L]}{(\bar{\xi}^2 - \beta^2 z^2)^{1/2}} \right) \right\} d\bar{\xi} \quad \text{(A13)}$$

$$\bar{v}(x,y,z) = -\frac{1}{\pi} \int_{\beta(y^2+z^2)^{1/2}}^{x} \frac{e^{-ik\bar{\xi}}}{[\bar{\xi}^2 - \beta^2(y^2 + z^2)]^{1/2}} \times \left\{ J_0 \left[\frac{\bar{k}}{M} (\bar{\xi}^2 - \beta^2 z^2)^{1/2} \right] + 2 \sum_{r=1}^{\infty} (-1)^r J_{2r} \times \left[\frac{k}{M} (\bar{\xi}^2 - \beta^2 z^2)^{1/2} \right] \cos \left(2r \sin^{-1} \frac{\beta y}{(\bar{\xi}^2 - \beta^2 z^2)^{1/2}} \right) \right\} d\bar{\xi} + \int_{\bar{\xi}_{00}}^{x} \frac{e^{-ik\bar{\xi}}}{\{(L^2 - \beta^2)\bar{\xi}^2 + 2\beta^2(x - Ly)\bar{\xi} - \beta^2[(x - Ly)^2 + L^2 z^2]\}^{1/2}} \times \left\{ J_0 \left[\frac{\bar{k}}{M} (\bar{\xi}^2 - \beta^2 z^2)^{1/2} \right] + 2 \sum_{r=1}^{\infty} (-1)^r J_{2r} \times \left[\frac{\bar{k}}{M} (\bar{\xi}^2 - \beta^2 z^2)^{1/2} \right] \cos \left(2r \sin^{-1} \frac{\beta[y - (x - \bar{\xi})/L]}{(\bar{\xi}^2 - \beta^2 z^2)^{1/2}} \right) \right\} d\bar{\xi} \quad \text{(A14)}$$

During evaluation of the integrals in (A13) and (A14), special measures must be taken to account for the integrably-singular behavior of the denominator radical of each integral at the lower limit. The procedure for so doing is well known.

Finally, it is remarked that the interesting relationship

$$\bar{\varphi} = x\bar{u} + y\bar{v} + z\bar{w} \quad \text{(A15)}$$

which was pointed out by Woodward in steady flow, is believed also valid in the oscillatory case.

References

[1] Landahl, M. T., "Pressure Loading Functions for Oscillating Wings with Control Surfaces," *AIAA Journal*, Vol. 6, No. 2, Feb. 1968, pp. 345–348.

[2] Van Dyke, M. D., *Perturbation Methods in Fluid Mechanics*, Academic Press, New York, 1964.

[3] Andrew, L. V., *Subsonic Generalized Forces on Aerodynamically Interfering Surfaces*, Rept. NA-69-904, July 1970, North American Rockwell Corp.

[4] Küssner, H. G., "Research on the Oscillating Elliptic Lifting Surface in Subsonic Flow," AFOSR-TR-60-71, June 1960, U.S. Air Force.

[5] Ashley, H., *Subsonic Oscillatory or Steady Airloads on Wings with Control Surfaces and Other Discontinuities*, AFOSR 68-0419, Dec. 1967, U.S. Air Force; also SUDAAR 336, Stanford Univ.

[6] Ashley, H. and Rowe, W. S., "On the Unsteady Aerodynamic Loading of Wings with Control Surfaces," *Zeitschrift für Flugwissenschaften*, Vol. 18, No. 9/10, Sept./Oct. 1970, pp. 321–330.

[7] Lagerstrom, P. A. and Graham, M. E., *Linearized Theory of Supersonic Control Surfaces*, Rept. SM13060, 1947, Douglas Aircraft Co.

[8] Berman, J. H., Skyprykevich, P., Smedfjeld, J. B., and Kelly, R. F., *Unsteady Aerodynamic Forces for General Wing/Control-Surface Configurations in Subsonic Flow*, AFFDL TR-67-117, 1968, Air Force Flight Dynamics Lab., Wright-Patterson Air Force Base, Ohio.

[9] Ashley, H. and Landahl, M. T., *Aerodynamic of Wings and Bodies*, Addison-Wesley, Reading, Mass., 1965.

[10] Brown, S. N. and Stewartson, K., "Flow Near the Apex of a Plane Delta Wing," *Journal of the Institute of Mathematics & Applications*, Vol. 5, 1969, pp. 200–216.

[11] Rodemich, E. R., "Analytic Solution of an Interference Problem in Supersonic Flow," Rept. SID 65-695, June 1965, North American Aviation.

[12] Moore, M. and Andrew, L. V., *Unsteady Aerodynamics for Advanced Configurations*, FDL-TDR-64-152, Pts. IV and VI, 1965 and 1967, Air Force Flight Dynamics Lab., Wright-Patterson Air Force Base, Ohio.

[13] Milne-Thompson, L. M., *Theoretical Hydrodynamics*, 4th ed., Macmillan, New York, 1960.

[14] White, R. B. and Landahl, M. T., "Effect of Gaps on the Loading Distribution of Planar Lifting Surfaces," *AIAA Journal*, Vol. 6, No. 4, April 1968, pp. 626–631.

[15] Mykytow, W. J., *Application of Unsteady Aerodynamics Methods to Configurations with Interference*, paper presented to the 29th Meeting, AGARD Structures and Materials Panel, Istanbul, Oct. 1969.

[16] Laschka, B., "Zur Theorie der harmonisch schwingenden tragenden Fläche bei Unterschallanströmung," *Zeitschrift für Flugwissenschaften*, Vol. 11, No. 7, July 1963, pp. 265–292.

[17] Clevenson, S. A. and Leadbetter, S. A., *Measurements of Aerodynamic Forces and Moments at Subsonic Speeds on a Simplified T-Tail Oscillating in Yaw about the Fin Midchord*, TN 4402, 1958, NACA.

[18] Davies, D. E., *Generalized Aerodynamic Forces a T-Tail Oscillating Harmonically in Subsonic Flow*, Rept. Structures 295, May 1964, Royal Aircraft Establishment, Ministry of Aviation.

[19] Stark, V. J. E., *Aerodynamic Forces on a Combination of a Wing and a Fin Oscillating in Subsonic Flow*, Rept. TN 54, Feb. 1964, SAAB Aircraft.

[20] Zartarian, G. and Hsu, P. T., *Theoretical Studies on the Prediction of Unsteady Supersonic Airloads on Elastic Wings*, WADC TR 56-97, Pts. I and II, Dec. 1955 and Feb. 1956, Wright Air Development Center, Wright-Patterson Air Force Base, Ohio.

[21] Ashley, H., *Supersonic Airloads on Interfering Lifting Surfaces in Supersonic Flow*, Document D2-22667, 1962, Boeing Co.

[22] Woodward, F. A., "Analysis and Design of Wing-Body Combinations at Subsonic and Supersonic Speeds," *Journal of Aircraft*, Vol. 5, No. 6, Nov.-Dec. 1968, pp. 528–534.

[23] Donato, V. W. and Huhn, Jr., C. R., "Supersonic Unsteady Aerodynamics for Wings with Trailing Edge Control Surfaces and Folded Tips," AFFDL-TR-68-30, Aug. 1968, Air Force Flight Dynamics Lab., Wright-Patterson Air Force Base, Ohio.

[24] Albano, E., *Planar Doublet Lattice Method for Aerodynamic Forces*, Northrop Corp., Rept. NOR 68-147, Oct. 1968, Norair Div.

[25] Albano, E. and Rodden, W. P., "A Doublet-Lattice Method for Calculating Lift Distributions on Oscillating Surfaces in Subsonic Flows," *AIAA Journal*, Vol. 7, No. 2, Feb. 1969, pp. 279–285.

[26] Falkner, V. M., "The Calculation of Aerodynamic Loading on Surfaces of Any Shape," A.R.C. R.&M. 1910, Aug. 1943, Aeronautical Research Council, England.

[27] Goland, M., Luke, Y. L., and Dengler, M. A., "Theoretical Studies of the Effects of Aspect Ratio on Flutter," WADC TR 54-29, June 1954, Wright Air Development Center, Wright-Patterson Air Force Base, Ohio.

[28] Jones, W. P., "The Calculation of Aerodynamic Derivative Coefficients for Wings of Any Plan Form in Non-uniform Motion," A.R.C. R.&M. 2470, Dec. 1946, Aeronautical Research Council, England.

[29] Landahl, M. T. and Ashley, H., "Thickness and Boundary Layer Effects," Pt. II, *AGARD Manual on Aeroelasticity*, March 1969, Chap. 9.

[30] Djojodihardjo, R. H. and Widnall, S. E., "A Numerical Method for the Calculation of Nonlinear, Unsteady Lifting Potential Flow Problems," *AIAA Journal*, Vol. 7, No. 10, Oct. 1969, pp. 2001–2009.

[31] Andrew, L. V. and Stenton, T. E., "Unsteady Aerodynamics for Advanced Configurations, Pt. VII, Velocity Potentials in Non-Uniform Transonic Flow over a Thin Wing," FDL-TDR-64-152 Pt. VII, Aug. 1968, Air Force Flight Dynamics Lab.

[32] Kacprzynski, J. J., Ashley, H., and Sankaranarayanan, R., "On the Calculation of Unsteady Nonlinear Three-Dimensional Supersonic Flow Past Wings," *Journal of Basic Engineering*, Vol. 90, Ser. D, No. 4, Dec. 1968, pp. 581–595.

[33] Allen, H. J., General Theory of Airfoil Sections Having Arbitrary Shape or Pressure Distribution, Rept. 833, 1945, NACA.

[34] Tinling, B. E. and Dickson, J. K., "Tests of a Model Horizontal Tail of Aspect Radio 4.5 in the Ames Twelve-Foot Pressure Wind Tunnel," A9G13, 1949, NACA.

[35] Ashley, H., Widnall, S., and Landahl, M. T., "New Directions in Lifting Surface Theory," *AIAA Journal*, Vol. 3, No. 1, Jan. 1965, pp. 3–16.

[36] Landahl, M. T. and Stark, V. J. E., "Numerical Lifting-Surface Theory—Problems and Progress," *AIAA Journal*, Vol. 6, No. 11, Nov. 1968, pp. 2049–2058.

[37] Kariappa, and Smith, G. C. C., "Further Developments in Consistent Unsteady Supersonic Aerodynamic Coefficients," AIAA Paper 71-177, New York, 1971.